Investigation of organic scintillators for neutron-gamma noise measurements in a zero-power reactor

Flynn B. Darby, *Member, IEEE*, Oskari V. Pakari, *Member, IEEE*, Michael Y. Hua, *Member, IEEE*, Vincent Lamirand, *Member, IEEE*, Shaun D. Clarke, *Member, IEEE*, Andreas Pautz, and Sara A. Pozzi, *Fellow, IEEE*

Abstract—Noise measurements in light water reactor systems aid in generating validation data for integral point kinetic parameter predictions and generating monitoring parameters for reactor safety and safeguards. The CROCUS zero-power reactor has been used to support both efforts via measurements with thermal neutron detectors to observe neutron noise and inorganic scintillators to observe gamma noise. The cross-correlation of gamma and neutron noise has been investigated at CROCUS with separate gamma-only and neutron-only detectors. Organic scintillators, sensitive to both neutrons and gamma rays, can be used to cross-correlate gamma-ray and neutron noise with a single detector type. Herein, we present noise measurements using organic scintillators in a light-water, zero-power research reactor for the first time. We discuss data obtained with two 5.08 cm-length by 5.08 cm-diameter cylindrical trans-stilbene detectors and two 6-mm cubic scintillators – one trans-stilbene and one organic glass – set in the water reflector of CROCUS and outside the reactor vessel. The prompt neutron decay constant was estimated to be $\alpha_{\text{CPSD}} = (154 \pm 1) \, \text{s}^{-1}$ at 3 mW critical from the (γ, γ) signal, which agrees within one standard deviation overlap with previous measurements with CeBr$_3$ and simulation in Serpent 2. The (n,n) estimate of $\alpha_{\text{CPSD}} = (145 \pm 23) \, \text{s}^{-1}$ at 3 mW critical lacked precision but agreed within one standard deviation overlap with previous ^{235}U fission chamber estimates and simulation in Serpent 2. The 6-mm cubic scintillators were too inefficient to estimate α, but informed possible small-cell, high-volume detection systems to improve the (n,n) estimate capabilities. Based on the high precision estimate of α from the (γ, γ) CPSD signal we suggest the further development of theory to calculate β_{eff} and Λ from gamma-ray noise measurements and recommend gamma noise measurements for future simulation validation and as a method of reactor monitoring.

Index Terms—power spectral density, neutron noise, reactor noise, organic scintillators, pulse-shape discrimination

I. INTRODUCTION

NOISE measurements offer a powerful non-invasive technique to observe a given fissile system's kinetic param-

F. B. Darby, M. Y. Hua, S. D. Clarke, and S. A. Pozzi are with the Department of Nuclear Engineering and Radiological Sciences (NERS), University of Michigan, Ann Arbor, MI 48109 USA (e-mail: fdarby@umich.edu).

O. V. Pakari, V. Lamirand, and A. Pautz are with the Laboratory of Reactor Physics and Systems Behaviour, Ecole Polytechnique Fédérale de Lausanne, 1015 Lausanne, Switzerland and the Nuclear Energy and Safety Division, Paul Scherrer Institut, 5232 Villigen PSI, Switzerland. O. V. Pakari also actively works with NERS.

eters. The kinetic parameters encompass the coefficients of the differential equations describing the temporal behavior of a neutron population in a neutron multiplying medium. Previous work [1] has provided estimates of kinetic parameters for the CROCUS zero-power reactor using multiple detector types to observe the neutrons and gamma rays that arise from fission. Our work seeks to improve the detector toolkit by using a dual-particle-sensitive organic scintillator setup. This approach will detect both neutrons and gamma rays simultaneously and conduct dual-particle noise with a single detector type, reducing the complexity of the measurement system and potentially improving measurement capabilities.

The neutron noise equations are derived using the point kinetics assumptions, leading to a set of equations that can be solved cost-efficiently and, if the system indeed allows for the used assumptions, offer a precise predictor for time-dependent phenomena of neutron populations [2]. Noise measurements refer to a method to estimate the prompt decay constant, $\alpha = (\beta_{\text{eff}} - \rho)/\Lambda$ [3], [4] – where β_{eff} is the effective delayed neutron fraction, Λ is the mean neutron generation time, and ρ is the reactivity – via the analysis of time series signals from detection systems set close to a fissile system. More advanced neutron noise measurements can also include the determination of β_{eff} and Λ [5], [6]. These measurements can then be used for code validation [7], integral parameter databases [8]–[10], and potentially for nuclear data assimilation [11].

Beyond this, point kinetic parameters remain constant during steady-state operations, providing a potential verification metric for reactor operations. Past and current safeguarding of nuclear research reactors does not prescribe online monitoring by default [12], [13]. The frequent estimate of α in a research reactor from radiation measurements could provide a useful and reliable supplementary tool for operation monitoring and verification by corroborating a reactor's critical ($\rho = 0$), sub-critical ($\rho < 0$), or supercritical state ($\rho > 0$). These measurements are reliant on measuring correlations arising from the fission chain reaction and cannot be spoofed by non-multiplying neutron sources of similar intensity.

In the past, estimates of the prompt neutron decay constant from neutron noise measurements of the CROCUS zero-power reactor at critical ($\rho = 0$) were completed with thermal neutron detectors and inorganic scintillators [1], [5], [14], [15]. Power spectral density analysis (also known as Cohn-α [3]) was used to estimate α using the gamma-ray-sensitive inorganic scintillators (CeBr$_3$) and neutron-sensitive thermal neutron

detectors (^{235}U fission chambers) inside or in contact with the reactor core. The estimates compared well to simulated values using iterated fission probability (IFP) predictions in Serpent 2 [16], where the highest accuracy per unit measurement time was found with (γ,γ) correlations [17]. With adequate experimental precision below typical biases that are seen between nuclear data libraries (see Figure 1, comparing IFP simulation using either JEFF3.3 or ENDF/B-8.0), noise measurements may eventually inform nuclear data evaluation [8]. The α estimates ranged from 150 s^{-1} to 170 s^{-1} at critical in the CROCUS reactor as summarized from previous work in Figure 1. Gamma-ray noise estimates proved to be more precise and in one standard deviation agreement with simulated IFP values. Despite noise equations being derived based on the behavior of neutrons from fission, the gamma rays appear to carry the same temporal information. The nuclear data for neutrons from fission is more thoroughly evaluated than the nuclear data for gamma rays from fission (such as gamma rays per fission, or the energy spectrum), further motivating the investigation and improvement of gamma-ray noise measurements to enable a feedback loop back to gamma-ray nuclear data.
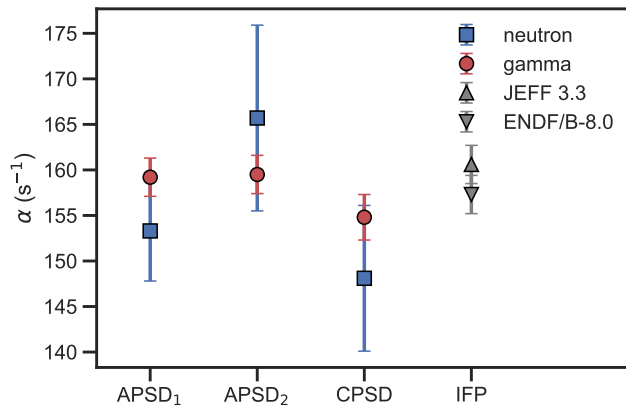

Fig. 1: Previous estimates of the prompt neutron decay constant (α) in CROCUS [1] leveraging CeBr$_3$ inorganic scintillators for gamma-ray detection, ^{235}U fission chambers for neutron detection, and the iterated fission probability (IFP) simulation method in Serpent 2. The APSD and CPSD methods are described in Section II-D. With the gamma-ray detectors, noise measurements became more precise than the differences in alpha estimates from simulation that arise from different nuclear data libraries (as shown here for JEFF3.3 or ENDF/B-8.0), we expect noise measurements to be able to contribute to databases for nuclear data evaluation and benchmarks.

In the previous works, neutron and gamma-ray noise were measured with neutron-only and gamma-only sensitive detectors. Notably, the detectors were set either into the control rod tubes in the core center, or very close to the fuel. In both cases, the detectors influenced the neutron economy of the reactor (and therefore also the reactor's prompt decay constant). This work uses organic scintillator measurements in the CROCUS zero-power reactor to leverage and investigate the potential benefits of, dual-particle sensitivity in a single detector volume for combined gamma-ray and neutron noise analysis. The organic scintillators in this work detect gamma-rays via Compton scattering and neutrons mainly via elastic scattering on hydrogen nuclei. Future work would benefit from the inclusion of organic scintillators with neutron capture capabilities, such as lithium or boron-loaded organic scintillators [18]–[20].

We set three trans-stilbene [21], [22] detectors and one organic glass (OGS) [23]–[25] detector deep in the CROCUS water reflector and outside the reactor vessel. Our work shows the successful application of organic scintillators for noise measurements in a light-water, zero-power research reactor for the first time. The detectors were well outside regions where they could measurably influence the neutron population in the reactor, thereby offering a potentially less biased estimate of α than previous experiments. This is important for simulation efforts to remain close to the benchmark configuration of CROCUS that is part of the International Reactor Physics Experiments Handbook (IRPhE) [26]. Additionally, looking at the potential application of noise measurements for international safeguards efforts, such as a "geometrically non-invasive" experiment, if successful, could pave the way towards a supplementary inspection tool for research reactors.

This paper is structured as follows. In Section II, we describe the CROCUS reactor II-A, the experimental setup II-B, organic scintillators and the pulse-shape discrimination technique II-C, and the power spectral density techniques II-D. We present and discuss estimates of the prompt neutron decay constant, α, calculated from our experiments in Section III. In the last Section IV, we discuss conclusions and future work based on our results.

II. METHODS

A. The CROCUS research reactor

The CROCUS zero-power research reactor is a two-region, water-moderated uranium core operated by the Laboratory for Reactor Physics and Systems Behaviour (LRS) at the Swiss Federal Institute of Technology Lausanne (EPFL). It is housed in a concrete shielding of about 1.3 m thickness, see Figure 2. It is a zero-power reactor, with a maximum power of up to 100 W. The reactor core is an approximately cylindrical configuration with a diameter of about 58 cm and a height of 100 cm, consisting of two fuel zones (see Figure 3). The central zone is loaded with 336 UO$_2$ fuel rods (1.806 wt.%-enriched), set in a square lattice with a pitch of 1.837 cm. The peripheral zone is loaded with up to 176 thicker, U$_{met}$ fuel rods (0.947 wt.%-enriched) with a pitch of 2.917 cm, also in a square lattice. The core is brought to criticality by introducing water from below via pumps, with an excess reactivity at the maximum water level being 200 pcm. The water level is controlled by a spillway that allows for 0.1 mm accuracy on the control of the water level (equivalent to about 0.4 pcm). The core is located in an aluminum water vessel, its diameter is 130 cm and its thickness is 1.2 cm [14].
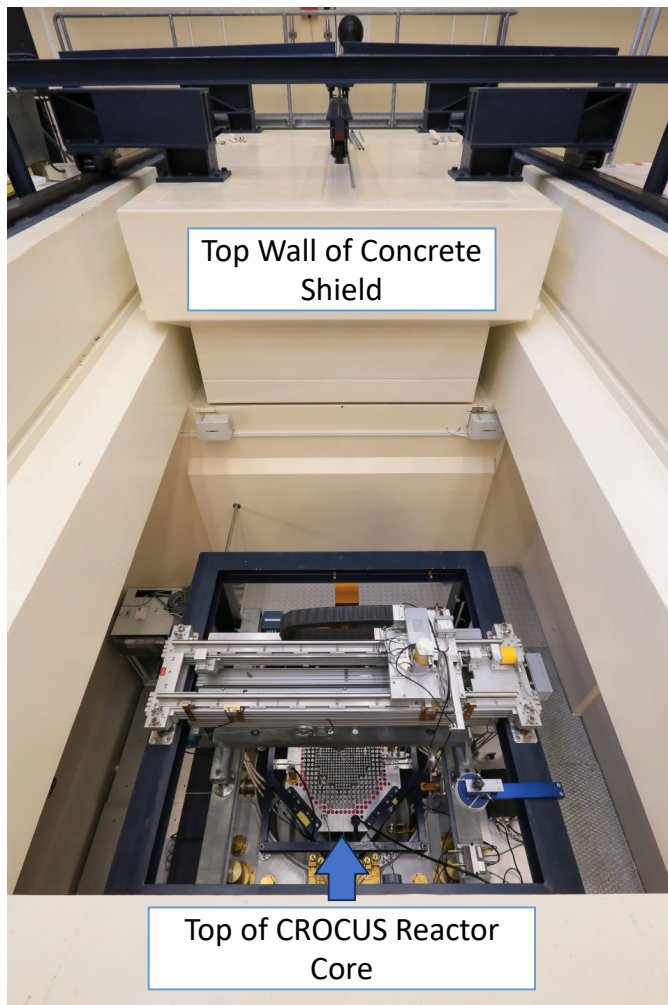
Fig. 2: Top-down view of the CROCUS reactor from above the concrete shield. The top wall may be opened when the reactor is shut down.

B. Neutron-gamma noise experimental setup

We placed two 5.08-cm-diameter by 5.08-cm-length trans-stilbene [21], [22] detectors in the water moderator offset 20 cm from the edge of the U_{met} zone and on the north (S2N) and east (S2E) sides of the reactor, as detailed in Figure 4a, with the active volume of each detector centered about the mid-height of the active fuel volume. A sealed, clear plastic tube fastened to the grid held the detector in position and protected the assembly from water. The detectors were connected to a CAEN DT5730S, 500-MHz, 14-bit digitizer and a CAEN DT1470ET high-voltage unit [22] in the reactor control room through diagnostic channels connecting the control room and containment while maximizing shielding. After a gradual search for the critical water level (959.3 mm), we measured the reactor for 120 minutes at 3 mW critical.

In a follow-up measurement, we moved these two detectors to positions outside the vessel on the north side (S2NW and S2NE) as shown in Figure 4b. The centers of the two detectors were 80 cm from the reactor core. Concurrently, we placed two 6-mm cubic detectors, one composed of trans-stilbene (S6E)
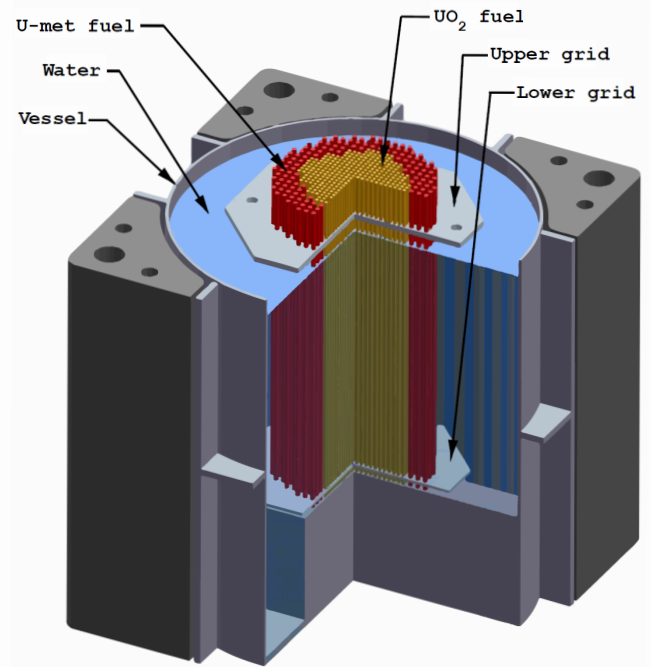

Fig. 3: Schematic view of the CROCUS reactor, showing the vessel, fuel grids, fuel elements, and water level when in operation.

and one composed of organic glass (O6N) [25], [27] as close as possible to the reactor core. We include the organic glass detector in our measurements due to the rising popularity and availability of organic glass and because trans-stilbene crystal detectors are currently unavailable to purchase from a vendor. After a gradual search for the critical water level (960.0 mm), we measured the reactor for 120 minutes at 20 mW critical.

Both detector configurations pose essentially no effect on the reactor kinetic state with positions in the water moderator and outside the vessel. Previous measurements introduced detectors in control rod positions and more fissile material (fission chambers) adjacent to the reactor core, posing direct effects on the neutron economy. The largest impact on the kinetic state of our experiment may be caused by the absence of water where the S6E and O6N detector tubes are located.

C. Organic scintillators and pulse-shape discrimination

Organic scintillators are dual-particle sensitive detectors. The hydrocarbon volume is sensitive to gamma rays mainly through Compton scattering on atomic electrons and sensitive to neutrons mainly through elastic scattering on hydrogen nuclei. Gamma-ray Compton scattering interactions cause free electron travel in the scintillator volume that deposits energy along a track length proportional to the energy of the Compton scatter. Neutron elastic scatter on hydrogen atoms cause proton tracks of much shorter length than energy equivalent electrons. Due to the higher stopping power of protons compared to electrons, a higher density of triplet excitation states occurs, resulting in a higher ratio of delayed fluorescence to prompt fluorescence. For this reason, the light output of neutron elastic
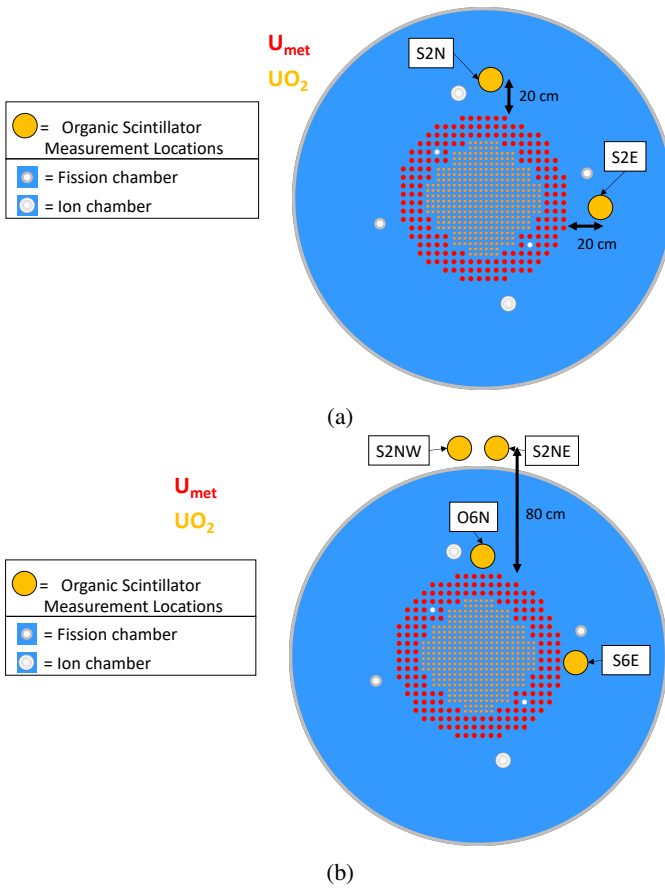
Fig. 4: Diagrammatic representations of axial cuts through the center height of the CROCUS reactor vessel highlighting the fuel grid, detector positions, and vessel boundary for each measurement. In (a) the first measurement, the two-inch (5.08 cm) trans-stilbene detectors are placed 20 cm from the edge of the U_{met} zones on the north (S2N) and east (S2E) sides of the reactor core in the CROCUS moderator. In (b) the second measurement, the two-inch (5.08 cm) trans-stilbene detectors are placed outside the CROCUS vessel (S2NW and S2NE), one 6 mm trans-stilbene detector is placed at the east edge of the core (S6E), and one 6 mm organic glass detector is placed at the north edge of the core (O6N).

scattering is delayed relative to energy-equivalent gamma-ray Compton scattering [28]–[30].

The difference in track length also warrants consideration of the detector geometry. A small detector of the same shape as a larger detector will have a higher surface area to volume ratio. The higher this ratio, the more likely scattered particles are to escape the detector volume. Because the electrons have a longer track length than protons, the leakage likelihood of electrons in a small volume is compounded, especially if the maximum dimension of the detector approaches the mean free path of the electrons. The same logic applies to the escape of scattered gamma rays and neutrons. This difference in leakage will cause gamma-ray interactions to have a decreased absolute light output and a higher relative decrease than equivalent neutron interaction light output [31]–[33].

We calibrate the light output of an organic scintillator using the Compton edge produced by a measured, mono-energetic (662-keV) ^{137}Cs source [22]. The detectors are calibrated by fitting the measured pulse-integral distribution for the Compton edge location (478 keV). When both collisions have equivalent energy deposition, the neutron light output from elastic scattering on hydrogen is less than the gamma-ray light output from Compton scattering [34]. For this reason, the detectors are only sensitive to fast neutrons. With a detection threshold of about 700 keV electron equivalent (keVee) this would equate to a 3 MeV neutron detection threshold [25], [29].

The incident neutron and gamma-ray radiation may be discriminated on the fly with charge-integration-based pulse-shape discrimination. By quantifying the delayed light output of neutrons in comparison to gamma rays, we discriminate between the two types of radiation. We quantify delayed light output with the tail over total ratio (R) defined as $R = \frac{\text{tail}}{\text{total}}$, where tail and total are pulse integral values defined diagrammatically in [22]. Neutron detections will generally have a higher ratio than equivalent light-output gamma-ray detections. We use optimal integral gates from [25] to obtain pulse-shape discrimination distributions.

D. Power spectral density technique

The time-dependent behavior of the neutron flux $n(t)$ can be described by the point kinetics approximation [2]:

$$\frac{dn(t)}{dt} = \frac{\rho(t) - \beta_{\text{eff}}}{\Lambda} n(t) + \sum_i \lambda_i c_i + S, \tag{1}$$

with the quantities ρ, the reactivity, β_{eff}, the effective delayed neutron fraction and Λ, the prompt generation time. The beta-delayed neutron precursor concentrations c_i and decay constants λ_i are derived via a balance equation, also known as the Bateman equation. The prompt neutron decay constant is defined as

$$\alpha = \frac{\beta_{\text{eff}} - \rho}{\Lambda}. \tag{2}$$

Using [35], the autocorrelation of a point-like reactor can be written as:

$$P_{ii}(\tau) = \frac{1}{2} Y \alpha e^{-\alpha|\tau|}, \tag{3}$$

with Y being

$$Y = \frac{\epsilon D_\nu}{(\beta_{\text{eff}} - \rho)^2}, \tag{4}$$

where ϵ is the detector efficiency in counts (C_i) over fission rate (F_0), and D_ν is the Diven factor [36]. When accounting for the overlap of uncorrelated fission chains, an autocorrelation term $\delta(\tau)$ needs to be added, here neglecting delayed neutrons for illustrative purposes [17]:

$$P_{ii}(\tau) = \epsilon F_0 \cdot \left(\frac{1}{2} Y_1 \alpha e^{-\alpha|\tau|} + \delta(\tau) \right). \tag{5}$$

This formulation, called the "Rossi-α method", is a common noise analysis technique using time interval distributions [4],

[37]. It describes the correlation of a given detection with one later in time. The $e^{-\alpha|\tau|}$ term is linked to the prompt fission chain, i.e., detecting a coincident neutron in a short time delay (τ) will have a higher likelihood than a coincidence in a longer time delay to stem from the same fission chain. The prompt fission chain will eventually terminate - thus, the name prompt decay constant for the coefficient of the exponential term. The remaining $\delta(\tau)$ accounts for the uncorrelated, constant time coincidences with respect to the time delay.

The auto power spectral density method (APSD) is an arguably more robust method to estimate α. The technique takes advantage of the frequency domain to focus on the cutoff frequency directly corresponding to the prompt neutron decay constant. The APSD of a detector is found by Fourier-transforming the Rossi-α function, yielding a Lorentzian [17]:

$$G_{ii}(\omega) = \int_{-\infty}^{\infty} dt \cdot e^{-i\omega t} P_{ii}(t) =$$
$$\epsilon_i F_0 + \frac{\epsilon_i^2 F_0 D_\nu}{(\beta_{\text{eff}} - \rho)^2} \frac{1}{1 + \omega^2/\alpha^2}. \quad (6)$$

By Fourier transforming the time series of a detector signal, one may directly fit this expression to obtain α, in this case not an exponential decay, but the Fourier transform of it: a Lorentzian bell curve with cut-off frequency ($f_c = \frac{\alpha}{2\pi}$).

The cross power spectral density (CPSD) similarly develops from the cross-correlation of two detectors, which theoretically removes the white noise [38], [39]:

$$G_{ij}(\omega) = \int_{-\infty}^{\infty} dt \cdot e^{-i\omega t} P_{ij}(t) = \frac{\epsilon_i \epsilon_j F_0 D_\nu}{(\beta_{\text{eff}} - \rho)^2} \frac{1}{1 + \omega^2/\alpha^2}. \quad (7)$$

Both APSD and CPSD are fit with the same function:

$$G_{ij}(\omega) = A + \frac{B}{1 + f^2/f_c^2}. \quad (8)$$

The constant "A" represents the white noise in both APSD and CPSD. Theoretically, the CPSD distribution would plateau to zero intensity at high frequencies, but in reality, there remains some white noise. The uncertainty in α is estimated from a trust region non-linear least squares fit using the variance term for the α parameter in the fit covariance matrix.

III. RESULTS AND DISCUSSION

The pulse-shape discrimination heatmaps in Figure 5 contrast the discrimination quality of our three types of detectors. S2E shows two distinct neutron and gamma-ray bands at high (≈ 0.25) and low (≈ 0.15) tail over total ratios. The two bands are distinct over all measured energies due to the high threshold (about 500 keVee). The heatmap has a dual color scale, where notably the signals classified as neutrons are two orders of magnitude less frequent than signals classified as gamma rays. Additionally, pulse-pileup caused by the intense gamma-ray flux is visible spanning across both bands. All pulses with $R > 0.2$ are classified as neutrons and all pulses with $R < 0.2$ are classified as gamma rays. The pulse-pileup

is most significant in the neutron band, where the band has cells of about 10^3 counts, but at low energies, the surrounding pile-up cells can reach about 10^2 counts. For the east 6 mm trans-stilbene detector in the second measurement (S6E) the pulse shape discrimination is quite similar to S2E, except the neutron and gamma-ray bands have higher respective ratios (about 0.35 and 0.15 respectively) and separation, the pulse-pileup is significantly reduced, and the discrimination line is $R = 0.25$. Also of note is the maximum light output for the small detector is lower due to the leakage of scattered particles and the neutron band is only one order of magnitude lower in intensity than the gamma-ray band. The O6N detector pulse-shape discrimination heatmap also has minimal pulse-pileup, the two bands are broader, the separation between the two bands is reduced with neutron and gamma-ray band ratios of about 0.32 and 0.22 respectively, and the discrimination line is $R = 0.28$.

The resultant auto power spectral density (APSD) distribution from the east detector yields a precise estimate of $\alpha = (155.6 \pm 1.4)$ s^{-1} when fit with equation 8 (see Figure 6a) without pulse-shape discrimination (note the majority of signal is gamma-rays). When considering only the signals classified as neutrons, the estimate is $\alpha = (247.1 \pm 58.7)$ s^{-1} (see Figure 6b). The neutron-only APSD is far less precise and the mean value is not near the expected value. The relative dispersion over the neutron APSD is much higher and the relative change in intensity over the neutron APSD is far lower than the gamma-ray APSD. Both factors decrease the accuracy of alpha from the Lorentzian fit. The main cause of this result is the difficulty of detecting fast neutrons in a thermal, water-moderated environment. More than 10 cm of water between the reactor core and our detectors greatly reduced our neutron signal relative to our gamma-ray signal. It should also be noted that the gamma-ray signal causes pulse pile-up that pollutes the neutron classification. The gamma-ray pulse pile-up could introduce interference in the true neutron signal that deteriorates the expected Lorentzian APSD shape.

Correspondingly, we summarize APSD α estimates of interest in Table I. All estimates from S2E, S2N, S2NW, and S2NE are precise and in agreement without pulse-shape discrimination and when analyzing the gamma-only signal. The neutron-only estimates for S2E and S2N widely disagree and S2NW and S2NE are near or within uncertainty of zero. The second measurement had approximately three times more water between the reactor and "S2" detectors, meaning that S2NW and S2NE were far less efficient on the neutron signal than S2E and S2N, leading to worse neutron-only APSD estimates. The S6E and O6N detectors are not included in the tabulated estimates because all estimates were within three standard deviations of zero. These detector volumes were too small to be sensitive to fission noise in the S6E and O6N positions.

TABLE I: APSD α estimates (s^{-1})

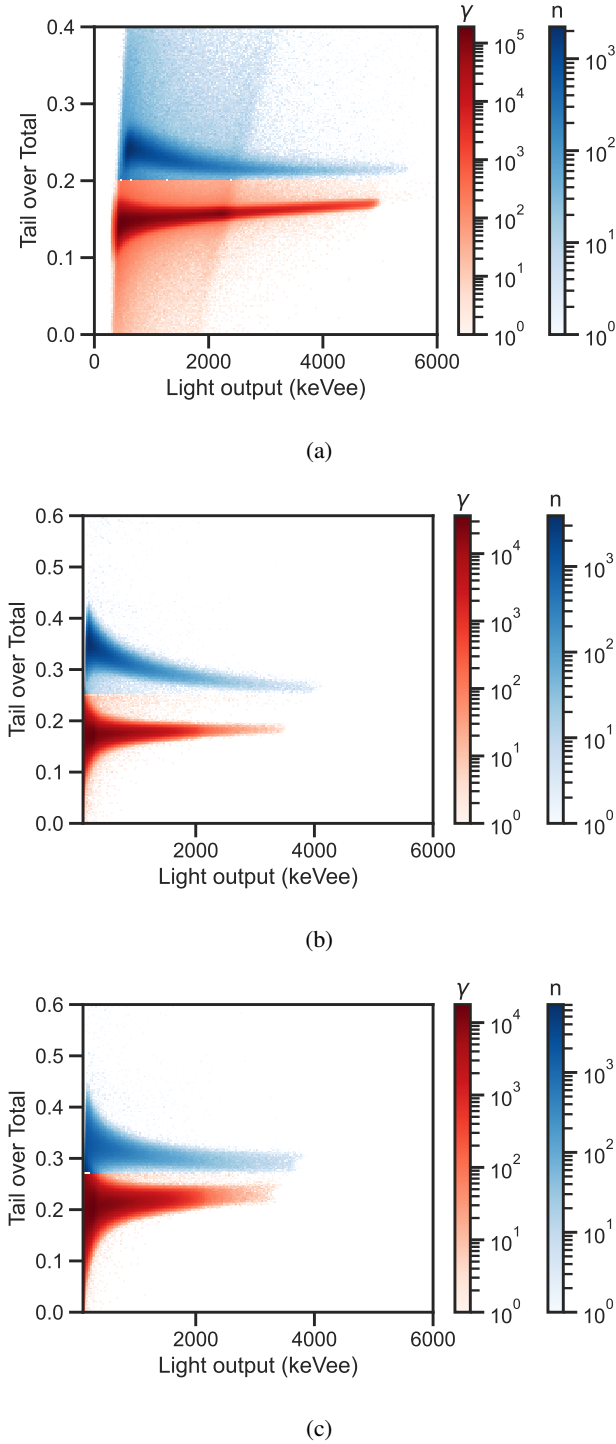|	S2E	S2N	S2NW	S2NE
All	155.6 ± 1.4	157.4 ± 1.4	153.8 ± 6.3	157.5 ± 4.9
γ	155.7 ± 1.5	157.3 ± 1.5	154.1 ± 6.5	156.7 ± 4.9
n	247.1 ± 58.7	101.6 ± 20.5	21.4 ± 9.8	19.1 ± 23.6

(a)

(b)

(c)

Fig. 5: Pulse-shape discrimination heat maps of tail over total ratios against the total light output in keV-electron-equivalent for a) S2E, b) S6E, and c) O6N detectors. The color values are in counts per heatmap cell. The ratio values above 0.2, 0.25, and 0.28 are taken to be neutrons and below are taken to be gamma-rays for the S2E, S6E, and O6N detectors respectively.

The cross power spectral density (CPSD) estimate using the S2E and S2N detectors is $\alpha = (154.0 \pm 1.0)$ s^{-1}, which is more precise than the corresponding APSD estimates. The

CPSD distribution (Figure 6c) has less dispersion than the APSD (Figure 6a), improving the fit precision. The neutron-only CPSD estimate is $\alpha = (145.4 \pm 23.1)$ s^{-1}, which is far less precise than the total CPSD, but does come within one standard deviation of the total estimate. It should be noted again that the gamma-ray pulse pile-up significantly pollutes the neutron classified signals. We also applied CPSD to the S2NW and S2NE pair. The total and gamma-only values of about $\alpha = (143 \pm 3)$ s^{-1} are lower than the S2E and S2N CPSD. The neutron-only value for S2NW and S2NE was not discernible due to the low neutron efficiency (indicated by the low intensity in Figure 6d). S6E and O6N showed no discernible frequency distribution beyond white noise because of their low efficiency leading to a lack of sensitivity to noise. All non-zero CPSD estimates are summarized in Table II.

TABLE II: CPSD α estimates (s^{-1})

All S2E/S2N	154.0	$\pm$	1.0
All S2NW/S2NE	144.0	$\pm$	3.4
(γ,γ) S2E/S2N	154.2	$\pm$	1.0
(γ,γ) S2NW/S2NE	143.4	$\pm$	3.4
(n,n) S2E/S2N	145.4	$\pm$	23.1

The gamma-only estimates with the S2E/S2N and S2NW/S2NE pairs are compared to previous estimates with CeBr$_3$ and simulated Serpent 2 iterated fission probability (IFP) in Figure 7a. The S2E/S2N pair gamma-only estimates are in excellent agreement with the previously calculated values and the precision is similar to the CeBr$_3$ measurements in-core in the control rod tube positions. The S2NW/S2NE pair gamma-only estimate agrees with the previous APSD estimates, but the CPSD estimate is just outside of one standard deviation agreement. Nevertheless, we have provided promising and comparable estimates for gamma noise without the need to place detectors in the reactor core. These results are less invasive and simpler to implement.

The neutron-only estimates are compared for the S2E/S2N to previous work in Figure 6d. The APSD estimates for the pair do not agree, but confine ^{235}U fission chamber values. The S2E/S2N neutron-only CPSD estimate agrees with the 235U fission chamber value, but the S2E/S2N has quite high uncertainty in comparison.

IV. CONCLUSIONS AND FUTURE WORK

Our results provide new estimates of the prompt neutron decay constant, α, of CROCUS at criticality in two 120-minute measurements. We notably used organic scintillators to estimate α at a far offset of 20 cm from the reactor core, demonstrating the effectiveness of organic scintillators for noise measurements for the first time.

In an attempt to prove dual-particle noise in a moderated reactor spectrum, the fast neutron signal collected by our detectors was insufficient to conduct power spectral density (PSD) analysis reliably on the neutron noise. Nonetheless, the neutron-only cross-PSD (CPSD) estimate of α was close to the expected value and merely lacked precision. However, to improve neutron estimates with organic scintillators, the possible deployment of lithium or boron-loaded organic scintillators could improve the neutron/gamma-ray signal ratio and
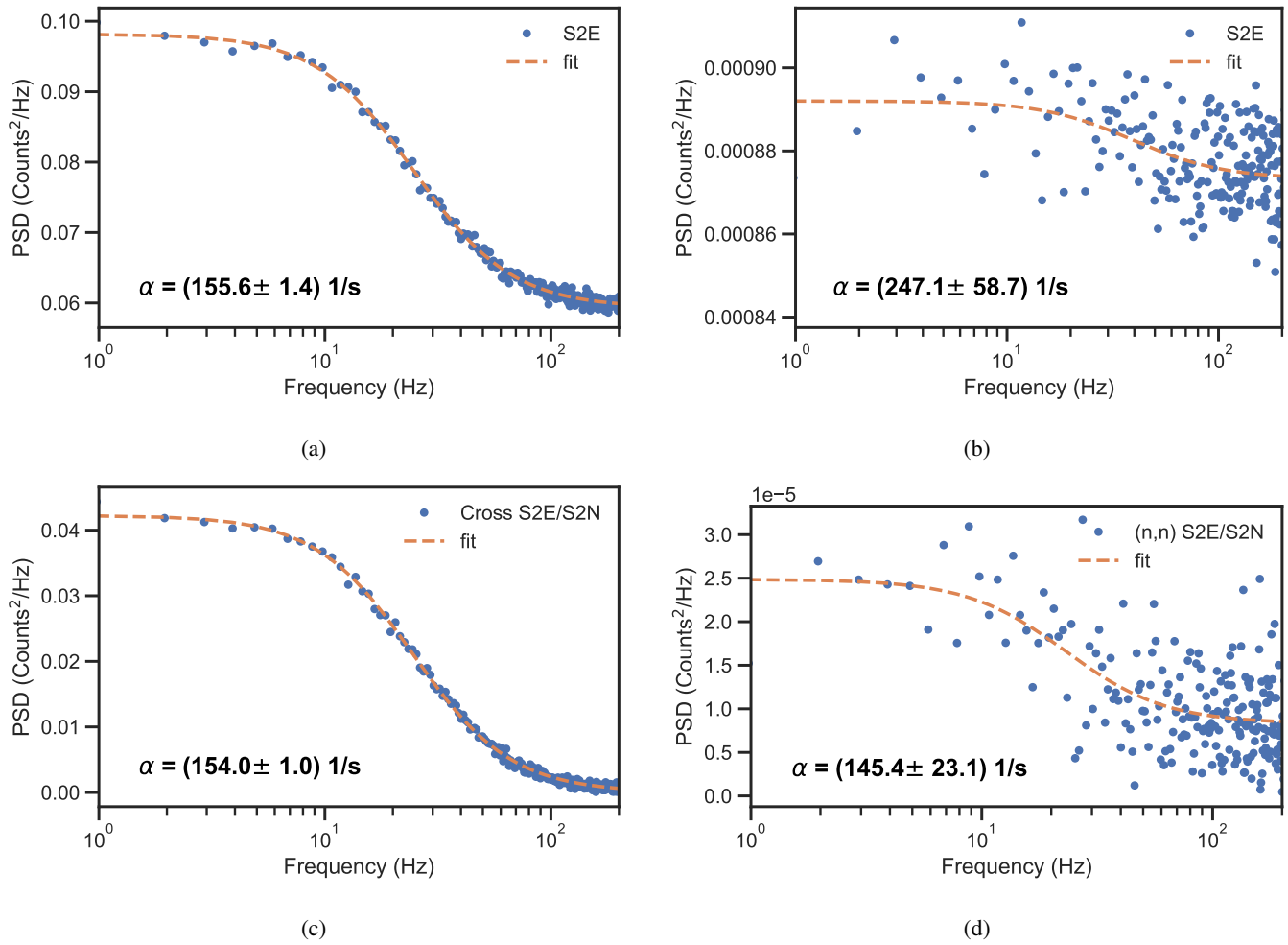
Fig. 6: The auto power spectral density (APSD) distributions of S2E for a) all pulses and b) neutron classified pulses alongside the cross power spectral density distributions of S2E/S2N for c) all pulses and d) neutron classified pulses. All distributions are generated from a 120-minute measurement at 3 mW critical.
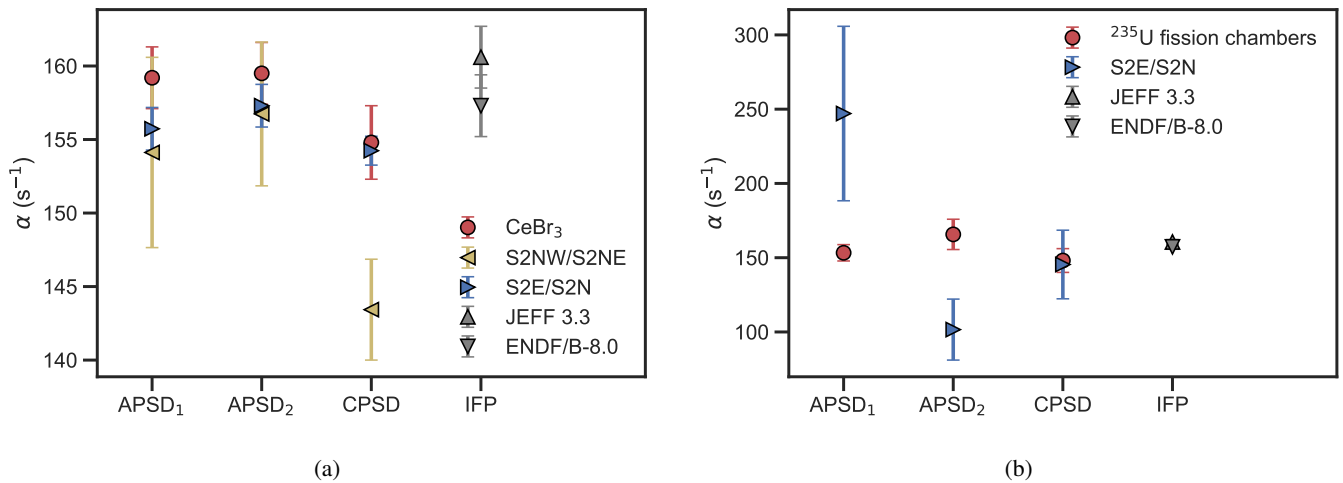

Fig. 7: α estimates from this work using the S2E/S2N and S2NW/S2NE pairs compared to previous estimates of the prompt neutron decay constant (α) from [1]. In a) our gamma noise results are compared to previous results from CeBr$_3$ inorganic scintillators and in b) our neutron noise results are compared to previous results from ^{235}U fission chambers. All results are compared to previously calculated α values from the iterated fission probability (IFP) simulation method in Serpent 2.

improve neutron-only CPSD estimates of α. By improving the neutron signal collection, we could add yet another mode of noise analysis to the evaluation toolkit.

The gamma-ray noise measurements compare well to previous measurements and simulations [1], [5], [16], [40]. The precise estimates from the gamma-ray noise motivate the future calculation of β_{eff} and Λ in CROCUS from gamma-only CPSD. The current equations used for power spectral density fitting to calculate β_{eff} and Λ are derived for the neutron population only [6], [41], [42] and leverage neutron nuclear data. Noise methods based on the gamma-ray signal have been briefly explored via theory and experimentation [43], [44], but there is an absence of theoretical development for the power spectral density technique leveraging gamma-ray noise, and the determination of β_{eff} and Λ from such signals. To calculate β_{eff} and Λ with the gamma-ray noise, a re-evaluation of the power spectral density equation derivation and use of gamma-ray nuclear data is required and encouraged.

Our estimates of α from the gamma-ray noise for CROCUS are a reliable and consistent reactor monitoring metric. The detector configurations in the water moderator and outside the vessel pose essentially no effect on the core kinetic state and do not require reconfiguration of the reactor core. Given minimal perturbation in the system, α is constant during steady-state critical operation in zero-power systems. Thus, monitoring α can serve to verify the kinetic state of a reactor. We propose using frequent monitoring of α during reactor operation to verify a reactor's kinetic state and facility activities, supplementing the international safeguards toolkit.

REFERENCES

[1] O. V. Pakari, V. Lamirand, T. Mager, P. Frajtag, and A. Pautz, "High accuracy measurement of the prompt neutron decay constant in CROCUS using gamma noise and bootstrapped uncertainties," *Annals of Nuclear Energy*, vol. 170, p. 109 011, Jun. 1, 2022, ISSN: 0306-4549. DOI: 10.1016/j.anucene.2022.109011. [Online]. Available: https://www.sciencedirect.com/science/article/pii/S0306454922000469 (visited on 05/25/2023).

[2] K. O. Ott and R. J. Neuhold, *Introductory nuclear reactor dynamics*. American Nuclear Society, 1985.

[3] C. E. Cohn, "Determination of reactor kinetic parameters by pile noise analysis*," *Nuclear Science and Engineering*, vol. 5, no. 5, pp. 331–335, May 1, 1959, Publisher: Taylor & Francis _eprint: https://doi.org/10.13182/NSE59-A25605, ISSN: 0029-5639. DOI: 10.13182/NSE59-A25605. [Online]. Available: https://doi.org/10.13182/NSE59-A25605 (visited on 09/30/2023).

[4] M. Y. Hua, F. B. Darby, J. D. Hutchinson, G. E. McKenzie, S. D. Clarke, and S. A. Pozzi, "Validation of the two-region rossi-alpha model for reflected assemblies," *Nuclear Instruments and Methods in Physics Research Section A: Accelerators, Spectrometers, Detectors and Associated Equipment*, vol. 981, p. 164 535, Nov. 21, 2020, ISSN: 0168-9002. DOI: 10.1016/j.nima.2020.164535. [Online]. Available: https://www.sciencedirect.com/science/article/pii/S0168900220309323.

[5] O. Pakari, V. Lamirand, G. Perret, P. Frajtag, and A. Pautz, "Kinetic parameter measurements in the CROCUS reactor using current mode instrumentation," *IEEE Transactions on Nuclear Science*, 2018, Publisher: IEEE.

[6] B. Geslot, F. Mellier, A. Pepino, *et al.*, "Kinetic parameters of the GUINEVERE reference configuration in VENUS-f reactor obtained from a pile noise experiment using rossi and feynman methods," in *Advancements in Nuclear Instrumentation Measurement Methods and their Applications (ANIMMA), 2015 4th International Conference on*, IEEE, 2015, pp. 1–6.

[7] O. Pakari, D. Mancusi, O. Petit, A. Zoia, V. Lamirand, and A. Pautz, "Towards the validation of noise experiments in the CROCUS reactor using the TRIPOLI-4 monte carlo code in analog mode," in *PHYSOR 2020*, 2020.

[8] M. Salvatores, G. Palmiotti, G. Aliberti, *et al.*, "Methods and issues for the combined use of integral experiments and covariance data: Results of a NEA international collaborative study," *Nuclear Data Sheets*, vol. 118, pp. 38–71, 2014, Publisher: Elsevier BV. DOI: 10.1016/j.nds.2014.04.005.

[9] G. Aliberti, G. Palmiotti, M. Salvatores, *et al.*, "Nuclear data sensitivity, uncertainty and target accuracy assessment for future nuclear systems," *Annals of Nuclear Energy*, vol. 33, no. 8, pp. 700–733, May 1, 2006, ISSN: 0306-4549. DOI: 10.1016/j.anucene.2006.02.003. [Online]. Available: https://www.sciencedirect.com/science/article/pii/S03064549060002296 (visited on 09/28/2023).

[10] D. A. Rochman, E. Bauge, A. Vasiliev, H. Ferroukhi, and G. Perret, "Nuclear data correlation between different isotopes via integral information," *EPJ Nuclear Sciences & Technologies*, vol. 4, p. 7, 2018, Publisher: EDP Sciences, ISSN: 2491-9292. DOI: 10.1051/epjn/2018006. [Online]. Available: https://www.epj-n.org/articles/epjn/abs/2018/01/epjn170045/epjn170045.html (visited on 09/28/2023).

[11] D. J. Siefman, "Development and application of data assimilation methods in reactor physics," Ph.D. dissertation, Lausanne, EPFL, 2019. DOI: 10.5075/EPFL-THESIS-7525.

[12] B. D. Reid, G. A. Anzelon, and K. Budlong-Sylvester, "Strengthening IAEA safeguards for research reactors," Pacific Northwest National Lab. (PNNL), Richland, WA (United States), PNNL-25885, Sep. 1, 2016. DOI: 10.2172/1330299. [Online]. Available: https://www.osti.gov/biblio/1330299 (visited on 09/29/2023).

[13] G. Zuccaro-Labellarte and R. Fagerholm, "Safeguards at research reactors: Current practices, future directions," *International Atomic Energy Agency Bulletin (Austria)*, vol. 38, Dec. 1, 1996. [Online]. Available: https://www.osti.gov/etdeweb/biblio/458058 (visited on 09/29/2023).

[14] O. Pakari, V. Lamirand, G. Perret, L. Braun, P. Frajtag, and A. Pautz, "Current mode neutron noise measurements in the zero power reactor CROCUS," in *EPJ*

Web of Conferences, vol. 170, EDP Sciences, 2018, p. 04 017.

[15] O. Pakari, V. Lamirand, B. Vandereydt, *et al.*, "Design and simulation of gamma spectrometry experiments in the CROCUS reactor," in *ANIMMA, Portoroz, Slovenia*, 2019.

[16] J. Leppänen, M. Aufiero, E. Fridman, R. Rachamin, and S. van der Marck, "Calculation of effective point kinetics parameters in the serpent 2 monte carlo code," *Annals of Nuclear Energy*, vol. 65, pp. 272–279, Mar. 1, 2014, ISSN: 0306-4549. DOI: 10.1016/j.anucene.2013.10.032. [Online]. Available: https://www.sciencedirect.com/science/article/pii/S0306454913005628 (visited on 09/26/2023).

[17] O. V. Pakari, "Experimental and numerical study of stochastic branching noise in nuclear reactors," Ph.D. dissertation, Lausanne, EPFL, 2020. DOI: 10.5075/EPFL-THESIS-8336.

[18] N. J. Cherepy, R. D. Sanner, P. R. Beck, *et al.*, "Bismuth- and lithium-loaded plastic scintillators for gamma and neutron detection," *Nuclear Instruments and Methods in Physics Research Section A: Accelerators, Spectrometers, Detectors and Associated Equipment*, vol. 778, pp. 126–132, Apr. 1, 2015, ISSN: 0168-9002. DOI: 10.1016/j.nima.2015.01.008. [Online]. Available: https://www.sciencedirect.com/science/article/pii/S0168900215000261 (visited on 11/18/2023).

[19] I. A. Pawełczak, A. M. Glenn, H. P. Martinez, M. L. Carman, N. P. Zaitseva, and S. A. Payne, "Boron-loaded plastic scintillator with neutron-γ pulse shape discrimination capability," *Nuclear Instruments and Methods in Physics Research Section A: Accelerators, Spectrometers, Detectors and Associated Equipment*, vol. 751, pp. 62–69, Jul. 1, 2014, ISSN: 0168-9002. DOI: 10.1016/j.nima.2014.03.027. [Online]. Available: https://www.sciencedirect.com/science/article/pii/S0168900214003210 (visited on 11/18/2023).

[20] L. Q. Nguyen, G. Gabella, B. L. Goldblum, *et al.*, "Boron-loaded organic glass scintillators," *Nuclear Instruments and Methods in Physics Research Section A: Accelerators, Spectrometers, Detectors and Associated Equipment*, vol. 988, p. 164 898, Feb. 1, 2021, ISSN: 0168-9002. DOI: 10.1016/j.nima.2020.164898. [Online]. Available: https://www.sciencedirect.com/science/article/pii/S016890022031295X (visited on 11/18/2023).

[21] N. Zaitseva, A. Glenn, L. Carman, *et al.*, "Scintillation properties of solution-grown trans-stilbene single crystals," *Nuclear Instruments and Methods in Physics Research Section A: Accelerators, Spectrometers, Detectors and Associated Equipment*, vol. 789, pp. 8–15, Jul. 21, 2015, ISSN: 0168-9002. DOI: 10.1016/j.nima.2015.03.090. [Online]. Available: https://www.sciencedirect.com/science/article/pii/S0168900215004635.

[22] F. B. Darby, M. Y. Hua, O. V. Pakari, S. D. Clarke, and S. A. Pozzi, "Multiplicity counting using organic scintillators to distinguish neutron sources: An advanced teaching laboratory," *American Journal of Physics*, vol. 91, no. 11, pp. 936–945, Nov. 1, 2023, ISSN: 0002-9505. DOI: 10.1119/5.0139531. [Online]. Available: https://doi.org/10.1119/5.0139531 (visited on 10/27/2023).

[23] J. S. Carlson and P. L. Feng, "Melt-cast organic glasses as high-efficiency fast neutron scintillators," *Nuclear Instruments and Methods in Physics Research Section A: Accelerators, Spectrometers, Detectors and Associated Equipment*, vol. 832, pp. 152–157, Oct. 1, 2016, ISSN: 0168-9002. DOI: 10.1016/j.nima.2016.06.116. [Online]. Available: https://www.sciencedirect.com/science/article/pii/S0168900216306866 (visited on 11/18/2023).

[24] P. L. Feng and J. Carlson, "Mixed compound organic glass scintillators," U.S. Patent 10508233B1, Dec. 17, 2019. [Online]. Available: https://patents.google.com/patent/US10508233/en (visited on 11/18/2023).

[25] T. H. Shin, P. L. Feng, J. S. Carlson, S. D. Clarke, and S. A. Pozzi, "Measured neutron light-output response for trans-stilbene and small-molecule organic glass scintillators," *Nuclear Instruments and Methods in Physics Research Section A: Accelerators, Spectrometers, Detectors and Associated Equipment*, vol. 939, pp. 36–45, Sep. 21, 2019, ISSN: 0168-9002. DOI: 10.1016/j.nima.2019.05.036. [Online]. Available: https://www.sciencedirect.com/science/article/pii/S0168900219306680 (visited on 09/28/2022).

[26] J. M. Paratte, R. Früh, U. Kasemeyer, M. A. Kalugin, W. Timm, and R. Chawla, "A benchmark on the calculation of kinetic parameters based on reactivity effect experiments in the CROCUS reactor," *Annals of Nuclear Energy*, vol. 33, no. 8, pp. 739–748, 2006, Publisher: Elsevier BV. DOI: 10.1016/j.anucene.2005.09.012.

[27] L. M. Clark, T. E. Maurer, S. Marin, N. P. Giha, S. D. Clarke, and S. A. Pozzi, "Time and energy resolution of organic glass scintillators for radionuclide monitoring," in *2021 IEEE Nuclear Science Symposium and Medical Imaging Conference (NSS/MIC)*, ISSN: 2577-0829, Oct. 2021, pp. 1–4. DOI: 10.1109/NSS/MIC44867.2021.9875704. [Online]. Available: https://ieeexplore.ieee.org/abstract/document/9875704?casa_token=rU-xChrUHjkAAAAA:U7BXndSNPtyGIUyBLPQD3PMjEyE_Y-phF2MTRfllaMDooNQmD01AW4TDSOEsE7gVVx04iUV4 (visited on 09/29/2023).

[28] F. D. Brooks, R. W. Pringle, and B. L. Funt, "Pulse shape discrimination in a plastic scintillator," *IRE Transactions on Nuclear Science*, vol. 7, no. 2, pp. 35–38, Jun. 1960, Conference Name: IRE Transactions on Nuclear Science, ISSN: 2374-9814. DOI: 10.1109/TNS2.1960.4315733.

[29] J. Birks, *The Theory and Practice of Scintillation Counting*, First. Pergamon Press Ltd., 1964.

[30] N. P. Zaitseva, Carman, M. Leslie, A. M. Glenn, and A. N. Mabe, *Plastic Scintillators: Chemistry and Applications* (Topics in Applied Physics), M. Hamel, Ed. Cham: Springer International Publishing, 2021,

vol. 140, Chapter 2, 35-39, ISBN: 978-3-030-73487-9 978-3-030-73488-6. DOI: 10.1007/978-3-030-73488-6. [Online]. Available: https://link.springer.com/10.1007/ 978-3-030-73488-6 (visited on 09/02/2022).

[31] I. M. Martin, A. Bui-Van, and G. Vedrenne, "Monte carlo simulation of an organic scintillator response of gamma-ray spectra," *Nuclear Instruments and Methods*, vol. 95, no. 3, pp. 545–550, Sep. 1, 1971, ISSN: 0029-554X. DOI: 10.1016/0029-554X(71)90557-X. [Online]. Available: https://www.sciencedirect.com/science/ article/pii/0029554X7190557X (visited on 09/29/2023).

[32] B. J. Snyder and G. F. Knoll, "Calculated gamma ray photofractions for well-type scintillation detectors," *Nuclear Instruments and Methods*, vol. 40, no. 2, pp. 261–266, Mar. 1, 1966, ISSN: 0029-554X. DOI: 10.1016/0029-554X(66)90384-3. [Online]. Available: https://www.sciencedirect.com/science/article/pii/ 0029554X66903843 (visited on 09/29/2023).

[33] M. Ellis, C. Tintori, P. Schotanus, K. Duroe, P. A. Kendall, and G. Mini, "The effect of detector geometry on EJ-309 pulse shape discrimination performance," in *2013 IEEE Nuclear Science Symposium and Medical Imaging Conference (2013 NSS/MIC)*, ISSN: 1082-3654, Oct. 2013, pp. 1–6. DOI: 10.1109/NSSMIC.2013. 6829467. [Online]. Available: https://ieeexplore.ieee. org/document/6829467 (visited on 09/29/2023).

[34] S. Seltzer, *Stopping-powers and range tables for electrons, protons, and helium ions, NIST standard reference database 124*, 1993. DOI: 10.18434/T4NC7P. [Online]. Available: http://www.nist.gov/pml/data/ star/index.cfm (visited on 11/18/2023).

[35] M. M. R. Williams, *Random processes in nuclear reactors*. Elsevier, 2013.

[36] B. Diven, H. Martin, R. Taschek, and J. Terrell, "Multiplicities of fission neutrons," *Physical Review*, vol. 101, no. 3, p. 1012, 1956, Publisher: APS.

[37] V. Lamirand, G. De Izarra, A. Krása, *et al.*, "Intercomparison of neutron noise measurement systems in the CROCUS reactor," in *Proc. PHYSOR*, 2018.

[38] R. Boffy, G. Truchet, B. Geslot, G. d. Izarra, and A. Sardet, "Measurement of delayed neutrons in a thermal nuclear reactor by means of a long run pile noise experiment in sub-critical state," *EPJ Web of Conferences*, vol. 284, p. 15 003, 2023, Publisher: EDP Sciences, ISSN: 2100-014X. DOI: 10.1051/epjconf/ 202328415003. [Online]. Available: https://www. epj-conferences.org/articles/epjconf/abs/2023/10/ epjconf_nd2023_15003/epjconf_nd2023_15003.html (visited on 06/23/2023).

[39] N. M. Tuan, T. T. Vien, T. C. Su, T. Q. Duong, and T. T. Tram, "Rossi-alpha parameter measurement of dalat nuclear reactor by analysis of cross power spectral density obtained from two ion chambers," Vietnam Atomic Energy Commission, Nuclear Research Institute, Dalat, Vietnam VAEC-AR 08–5, 2010, p. 40.

[40] T. Mager, O. Pakari, V. Lamirand, and A. Pautz, "The LEAF system and gamma detection applications in CROCUS," Master's Thesis, École polytechnique fédérale de Lausanne (EPFL), Grenoble Phelma, and Politecnico di Torino, 2020.

[41] M. N. Moore, "The determination of reactor transfer functions from measurements at steady operation," *Nuclear Science and Engineering*, vol. 3, no. 4, pp. 387–394, Apr. 1, 1958, Publisher: Taylor & Francis _eprint: https://doi.org/10.13182/NSE58-A25476, ISSN: 0029-5639. DOI: 10.13182/NSE58-A25476. [Online]. Available: https://doi.org/10.13182/NSE58-A25476 (visited on 09/30/2023).

[42] O. Pakari, "Kinetic parameter uncertainty quantification for the power spectral density method in zero power noise analysis," 2019.

[43] D. Chernikova, S. F. Naeem, N. Trnjanin, K. Axell, and A. Nordlund, "Gamma rossi-alpha, feynman-alpha and gamma differential die-away concepts as a potential alternative/complement to the traditional thermal neutron based analysis in safeguards," *arXiv preprint arXiv:1507.05474*, 2015.

[44] M. Hua, J.-T. Iacovetta, S. Clarke, S. Pozzi, and D. Trimas, "Rossi-alpha measurements with organic scintillators using gamma rays and fast-neutrons," presented at the INMM 60th Annual Meeting, Palm Desert, CA: Institue of Nuclear Materials Management, Jul. 1, 2019.